

Determination of Flow Stress and Cutting Force Prediction of Ti-6Al-4V Material for 3D Printer using S-K Constitutive Equation

Dae-Gyoun Park^{*}, Tae-Ho Kim^{**,#}, Eon-Chan Jeon^{***}

^{*}Department of Mechanical Engineering, Graduate School, Dong-A UNIV.,

^{**}T&SMachining, ^{***}Department of Mechanical Engineering, Dong-A UNIV.

S-K 구성방정식을 이용한 3D 프린터용 Ti-6Al-4V 재료의 유동응력 결정 및 절삭력 예측

박대균^{*}, 김태호^{**,#}, 전언찬^{***}

^{*}동아대학교 기계공학과 대학원, ^{**}티엔에스머시닝, ^{***}동아대학교 기계공학과

(Received 26 June 2018; received in revised form 30 July 2018; accepted 16 September 2018)

ABSTRACT

Study on the Ti-6Al-4V have been carried out using cutting simulation, and researches for cutting force and chip shape prediction have been actively conducted under various conditions. However, a 3D printer application method using Ti-6Al-4V metal powder material as a high-power method has been studied for the purpose of prototyping, mold modification and product modification while lowering material removal rate. However, in the case of products / parts made of 3D printers using powder materials, problems may occur in the contact surface during tolerance management and assembly due to the degradation of the surface quality. As a result, even if a 3D printer is applied, post-processing through cutting is essential for surface quality improvement and tolerance management. In the cutting simulation, the cutting force and the chip shape were predicted based on the Johnson-Cook composition equation, but the shape of the shear type chip was not predictable. To solve this problem, we added a damaging term or strain softening term to the Johnson-Cook constitutive equation to predict chip shape. In this thesis, we applied the constant value of the S-K equations to the cutting simulation to predict the cutting force and compare with the experimental data to verify the validity of the cutting simulation and analyzed the machining characterization by considering conditions.

Key Words : S-K Constitutive Equation(S-K 구성방정식), Cutting Force(절삭력), Ti-6Al-4V(티타늄), Orthogonal machining(직교 절삭 가공), Cutting-Simulation(절삭시뮬레이션), Flow Stress(유동응력)

1. Introduction

The applications and uses of titanium alloys have

increased in aviation, space, and medical industries due to their superior mechanical properties such as high strength and corrosion resistance. However, since titanium alloys are difficult to cut, due to their low machinability when they are processed to

Corresponding Author : kth0110@gmail.com

Tel:+82-51-201-4048, Fax: +82-53-201-4041

produce major parts, their applications have been limited^[1]. To overcome this, a measure of a three-dimensional (3D) printer application using Ti-6Al-4V metal powder material with a high-power method has been studied to facilitate prototype production, mold modification, and product modification while reducing the material reduction rate. However, products or parts manufactured using 3D printers and powder materials have a contact surfaces problem during tolerance control and assembly, due to surface quality degradation. Consequently, it is necessary to have post-processing in the form of cutting machining on the product surface to improve surface quality and tolerance control even if 3D printers are applied.

With regard to studies on titanium cutting, Park et al^[2] measured cutting property and surface roughness of a Ti-6 Al-4V alloy using a TiAlN coating tool via PVD coating technology, and the authors observed the shape of chips produced during the cutting process thereby analyzing the chip processability. Kim^[3] observed cutting heat and tool wear generated during cutting machining according to cut depth and time in medium-speed rough cutting machining of titanium alloys. Kim et al^[4] configured a lathe cutting system of titanium alloy based on cryogenic cooling utilizing nano-fluid MQL and liquid nitrogen, and they designed six experiments that evaluated the characteristics of lathe cutting machining according to lubrication and cooling conditions. Furthermore, Kim et al^[1] performed a study in dry, cryogenic cooling, and material heating and cryogenic cooling conditions, thereby deriving the cutting load and frictional coefficient between tool and chip that occurred during machining and performing comparative analyses on the derived results by each condition. Ye et al^[5] performed a finite element analysis (FEA) using the tool modeled according to each shape parameter to identify the machining characteristics of a widely used Ti-6Al-4V alloy by

helix angle and rake angle (major shape parameters of end mill tools); the authors fabricated actual tools and evaluated machinability using those tools. However, few studies have been conducted on the application of a cutting simulation to Ti-6Al-4V.

A simulation has been developed based on FEA according to detailed machining methods. In particular, the demand on simulations for process analysis has increased steadily for material molding and machining, which includes plastic working. In particular, numerical analysis has been actively conducted with the development of computers in cutting machining, and cutting conditions, machinability evaluations, and cutting quality are now able to be predicted. However, work pieces receive severe deformation and shear during cutting machining at a very high strain, high speed, and high temperature. Thus, the physical property model used inside the cutting simulation should be a function of strain, strain rate, and temperature. In general, the Johnson–Cook model has been most universally used to describe the relationship between material flow stress and strain rate. The material flow stress is affected by work hardening, strain rate hardening, and softening temperature, which are not independent but correlated. The Johnson–Cook model has several problems in that it has a limited strain rate region that can be expressed in the test, it lacks the description of a sudden increase in flow stress at the strain rate hardening, and a small error in the test can become a large error in the cutting force prediction as the constant value is highly sensitive to the cutting force during cutting^[5].

Thus, this study aims to calculate a constant in the S–K constitutive model, apply this to cutting simulations to predict a cutting force, verify the effectiveness of the cutting simulation by comparing the predicted cutting force with experimental data by condition, and analyze the machining characteristics by condition.

2. S-K constitutive equation and determination of coefficient value

2.1 Constitutive equation

The material flow stress is affected by work hardening, strain rate hardening, and softening temperature. It is known that when a constitutive equation is made by separating these three phenomena, it can describe the material flow stress relatively accurately. The three phenomena are separated and considered by providing a strain rate-related dimensionless number that considers the effect of strain rate as well as a temperature-related dimensionless number that considers the temperature effect on the flow stress-effective strain relation between the strain rate and temperature, which become the reference parameters.

$$\sigma = [A + B(1 - \exp(-C\epsilon))] \cdot [D \ln(\dot{\epsilon}/\dot{\epsilon}_0) + \exp(E \cdot (\dot{\epsilon}/\dot{\epsilon}_0))] \cdot \left[1 - \frac{T - T_{ref}}{T_m - T_{ref}}\right]^m \quad \dots\dots(1)$$

Here, σ refers to flow stress, ϵ refers to effective plastic strain rate, $\dot{\epsilon}$ refers to strain rate, $\dot{\epsilon}_0$ refers to strain rate, T refers to temperature, T_m refers to melting temperature, T_{ref} refers to the reference temperature, and A, B, C, D, E, and m refer to material constants. In the equation, the exponent m is applied to the entire square bracket, which proves that it can describe data well even in a lower temperature than the reference temperature and display the temperature softening phenomenon effectively. Eq. (1) presents the S-K constitutive equation.

2.2 Experiment and results of Split Hopkins Pressure Bar (SHPB)

The principle and test method of the Split Hopkins Pressure Bar (SHPB) test device are as follows. First, when the input rod is hit by the output rod by moving the output rod at high speed, specimen compressive elastic waves are generated at the specimen located between input and output rods. Once the generated compressive elastic waves are then delivered to the inside of the input rod and arrive at the boundary between the specimen and input rod, some of the compressive waves are reflected by the impedance difference between the input rod and the specimen, and some are penetrated through the specimen and delivered to the output rod. This is shown in Fig. 1 [6][7].

To determine the effect of the strain rate on the dynamic strain behavior of the specimen material, experiments were conducted at 0.0001/s, 0.05/s, 1700/s, 2100/s, and 1800/s (342°C) of strain rate. In addition, to determine the effect of temperature

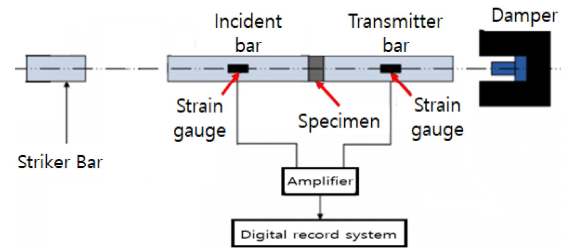


Fig. 1 Schematic of the SHPB device

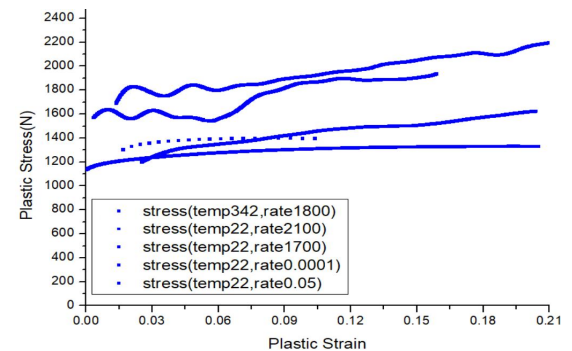


Fig. 2 Plastic strain-stress curve of Ti-6Al-4V each strain rate

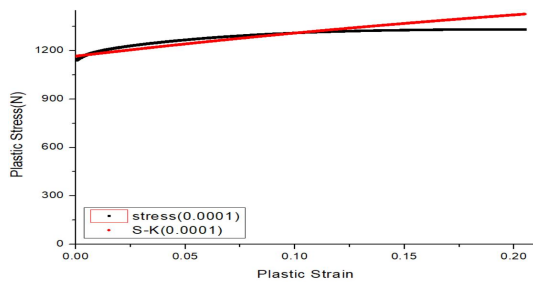
high-temperature tests were conducted at 342°C change on the dynamic strain behavior, and 1800/s of strain rate. Fig. 2 shows the true stress and strain curve, in which the stress value increases as the strain rate increases. This figure verifies that the stress value increases as the strain rate increases due to material hardening, and the stress value decreases as the temperature increases due to material softening.

2.3 Determination of coefficient value in the S-K constitutive equation

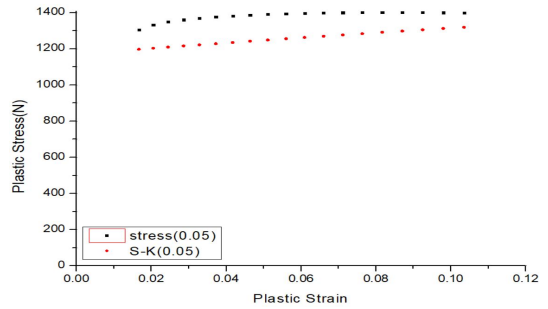
The coefficient value in the constitutive equation expresses the stress-strain (S-S) curve according to the reference strain rate, using the result values obtained through the SHPB experiment. This was acquired as the origin of the graph obtained through the SHPB experiment at room and high temperatures. A, B, C, D, and E values can be obtained using the graph acquired at a room temperature according to changes in strain rate, and value m can be calculated by changing temperature while the strain rate remains fixed.

Table 1 Parameter in the S-K constitutive equation

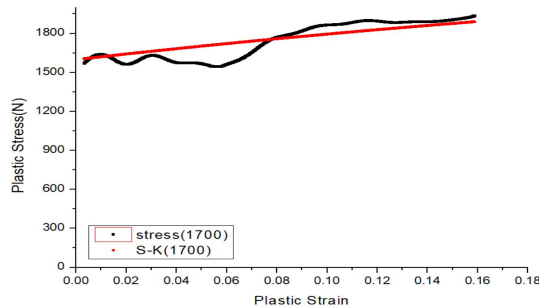
Parameter	Values
A(MPa)	1173.208
B(MPa)	681.817
C	2.372
D	0.00149
E	0.0001798
m	1.11457



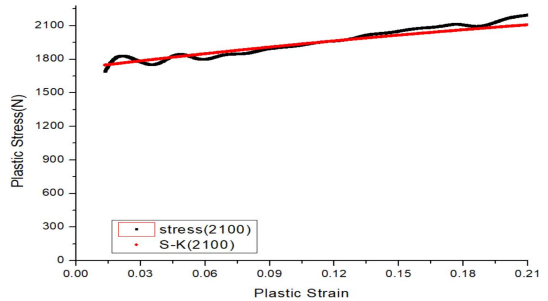
a) Rate 0.001, Temp 22°C



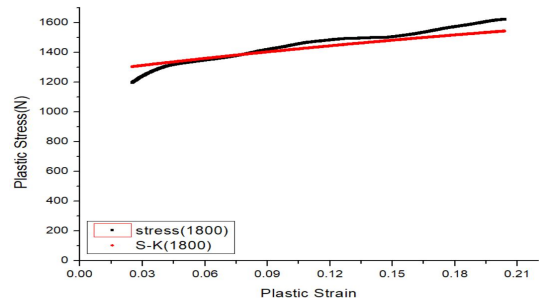
b) Rate 0.05, Temp 22°C



c) Rate 1700, Temp 22°C



d) Rate 2100, Temp 22°C



e) Rate 1800, Temp 342°C

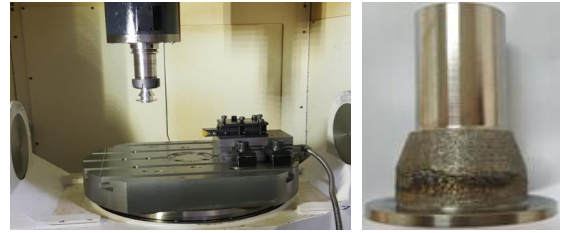
Fig. 3 Comparison of S-S curve of SHPB experiment and S-K constitutive equation with variation of strain rate

Table 1 presents the coefficient values in the S–K constitutive equation. The curve fitting result showed that the R2 value that expressed the accuracy of the data was 0.9711, which verified that the curve fitting was significant. Fig. 3 shows the result values in the S–K constitutive equation after applying the predicted coefficients and result values in the SHPB experiment according to changes in strain rate as a graph. The results of Fig. 3 verify that Fig. 3 a) shows that the predicted stress is higher than that of experiment whereas b), c), d), and e) show that the stress predicted by the S–K constitutive equation is lower than that of the experiment. This predicts that a cutting force in the cutting simulation will be lower than that of the experiment. The coefficient values of the correlation between the experiment and the S–K constitutive equation verified a positive correlation, as shown in 0.83 at 0.05 of the rate and 0.99 at 1,800 of the rate and 342 °C of temperature. The above results indicate that the S–S curve obtained by the S–K constitutive equation showed good matching with the data acquired through the experiment.

3. Comparison of the cutting test and simulation results

3.1 Orthogonal test device and conditions

Two-dimensional (2D) cutting tests were conducted to verify the cutting force predicted using the simulation. Fig. 4 shows the specimen for the cutting test and the 2D cutting test device using the machining center. The specimen was mounted in the rotational axis, and the tool was mounted and fixed to the tool dynamometer. Table 2 presents the cutting conditions that were applied to the cutting experiment and simulation. The cutting speed was increased from 40 m/min to 120 m/min with 40 m/min increments to have three conditions, and the feed rate was increased from 0.1 mm/rev to 0.2



a) experimental machine b) Specimen
Fig. 4 Specimens and experimental machine for cutting test

Table 2 Experimental condition of metal cutting

case	cutting speed (m/min)	feed rate (mm/rev)	depth of cut (mm)
case01	40	0.1	2
case02	40	0.15	
case03	40	0.2	
case04	80	0.1	
case05	80	0.15	
case06	80	0.2	
case07	120	0.1	
case08	120	0.15	
case09	120	0.2	

mm/rev with 0.05 mm/rev increments to have three conditions. The cut depth was fixed at 2 mm in the experiment and simulation.

3.2 Cutting simulation

A thermal structural softening AdvantEdge finite element model (FEM) at a plane strain rate in a 2D cutting machining was created and used. It was assumed that the elasto-plastic behavior of the workpiece was determined by flow stress according to strain, strain rate, and temperature. The Coulomb friction model was used for the model of the boundary between the chip and tool, and a quadratic triangular six-node shell element was used for the modeling element. Fig. 5 shows the cutting simulation process using AdvantEdge FEM. In the pre-process, cutting types were defined followed by shape, physical properties, and cutting machining conditions. The numerical analysis was conducted using the Third Wave Engine according to the defined

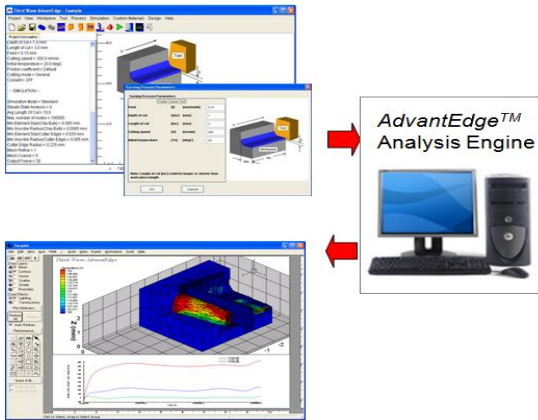


Fig. 5 Numerical analysis process of AdvantEdge

conditions, and the results were analyzed to obtain required data using Tech Plot.

3.3 Comparison of cutting force between simulation and cutting test

To compare and analyze the results data in the cutting experiment and simulation, the acquired data were curve-fitted in the cutting experiment and simulation thereby determining the mean value as the cutting force. Fig. 6 shows the cutting force acquired in the cutting experiment and the mean values based on the polynomial fitted graph of the acquired data. Fig. 7 shows the cutting force obtained in the simulation, and mean values are displayed based on the polynomial fitted graph of the data acquired by the simulation. Table 3 presents the cutting force results in the experiment and simulation by condition. The simulation cutting force results, compared to those of the experiment, showed that Fx cutting force can be predicted within 0.7% up to 7% by the cutting simulation, and Fy cutting force can be predicted within 2% up to 23%, which verified the difference that occurred during the fitting process. In addition, the validity of the cutting simulation can be verified based on the cutting experiment results. Fig. 8 shows the 2D cutting experiment and simulation results. The

comparison result of cutting forces between cutting experiment and simulation verified that the cutting force obtained by the simulation was higher than that of cutting experiment. It also verified that the cutting force increased as the feed rate increased at the same cutting speed, but the cutting force decreased as the cutting speed increased at the same feed rate.

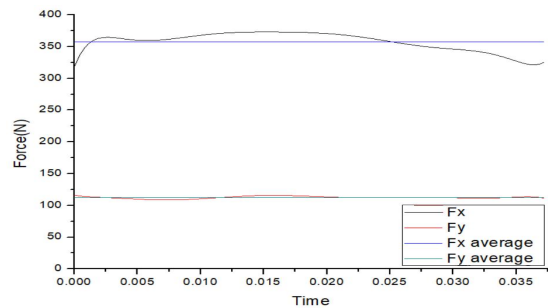


Fig. 6 2-Dimension experimental cutting force (case01)

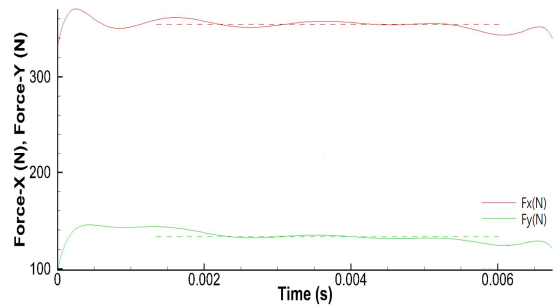


Fig. 7 2-Dimension simulation cutting force(case01)

Table 3 Comparison of experimental and simulation cutting forces by condition

case	simulation		experimental	
	Fx(N)	Fy(N)	Fx(N)	Fy(N)
case01	357.28	112.42	354.59	134.60
case02	477.86	123.14	496.37	139.73
case03	648.69	209.71	700.46	214.22
case04	349.51	126.68	361.03	145.75
case05	463.67	131.49	499.89	170.18
case06	612.44	250.58	621.95	212.88
case07	330.29	113.69	351.61	146.24
case08	435.71	183.09	469.44	186.22
case09	555.96	277.67	578.58	219.84

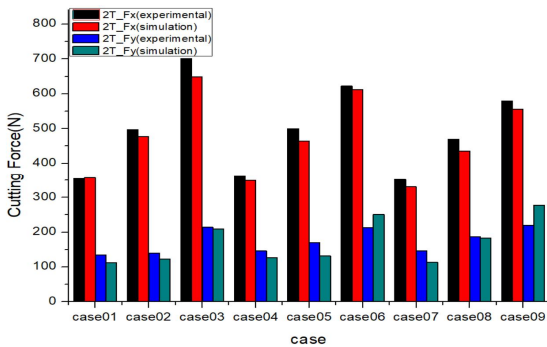


Fig. 8 Comparison of 2-Dimension experimental and simulation cutting force

4. Conclusions

This study aimed to calculate a constant in the S-K constitutive model, apply this to a cutting simulation to predict a cutting force, verify the effectiveness of the cutting simulation by comparing the predicted cutting force with experimental data by condition, and analyze the machining characteristics by condition. The study results can be summarized as follows:

1. The coefficient values in the S-K constitutive equation through the SHPB experiment were determined to be: A: 1173.208 MPa, B: 681.817 MPa, C: 2.372, D: 0.00149, E: 0.0001798, and m: 1.11457.
2. The simulation cutting force results, compared to those of the experiment, showed that the Fx cutting force can be predicted within 0.7% up to 7% by the cutting simulation, and Fy cutting force can be predicted within 2% up to 23%, but this difference was verified in that it occurred during the fitting process due to data falling below 0. In addition, the validity of the cutting simulation can be verified based on the cutting experiment results.
3. The results verified that the cutting force increased as the feed rate increased at the same cutting speed, but the cutting force was reduced

as the cutting speed increased at the same feed rate.

REFERENCES

1. Kim, J. W., Kim, J. S., Lee, S. W., "Experimental Characterization of Turning Process of Titanium Alloy Using Cryogenic Cooling and Nanofluid Minimum Quantity Lubrication", J. Korean Soc. Precis. Eng., Vol. 34, No. 3, pp. 185-189, 2017.
2. Park, J. N., Cho, G. J., Lee, S. C., "A Study on the Cutting Characteristics of Ti-6Al-4V Alloy in Turning Operation", Journal of the Korean Society of Manufacturing Process Engineers, Vol. 3, No. 4, pp.81~87, 2004.
3. Kim, G. H., "A Study on Characteristics of Cutting by Cutting Conditions in Titanium Machining", Journal of the Korean Society of Manufacturing Process Engineers, Vol. 12, No. 1, pp. 84-89, 2013.
4. Kim, D. Y., Kim, D. M., Park, H. W., "Study on Characteristics of Cryogenic Machining Process of Titanium Alloy at a Low Cutting Speed", J. Korean Soc. Precis. Eng., Vol. 34, No. 4, pp. 237-241, 2017.
5. Shin, H. h., Kim, J. B., "Description Capability of a Simple Phenomenological Constitutive Model for High-Strain-rate Plasticity Data", Proceedings of the Korean Society for Technology of Plasticity Conference, pp. 190-193, 2009.
6. An, W. J., Woo, M. A., Noh, H. G., Kang, B. S., Kim, J., "Design and Fabrication of Split Hopkinson Pressure Bar for Acquisition of Dynamic Material Property of Al6061-T6", Korean Society of Precision Engineering, Vol. 33, No. 7, pp. 587-594, 2016.
7. Park, D. G., Kim, T. H., Jeon, E. C., "Flow Stress Determination of Johnson-Cook Model of Ti-6Al-4V Material produce using 3D Printing Technique", Journal of the Korean Society of Manufacturing Process Engineers, Vol. 17, No. 4, pp. 64-69, 2018.